



**HAL**  
open science

# Evolution-driven versatility of N-terminal acetylation in photoautotrophs

Carmela Giglione, Thierry Meinell

► **To cite this version:**

Carmela Giglione, Thierry Meinell. Evolution-driven versatility of N-terminal acetylation in photoautotrophs. *Trends in Plant Science*, 2021, 26 (4), pp.375-391. 10.1016/j.tplants.2020.11.012 . hal-03011833

**HAL Id: hal-03011833**

**<https://hal.science/hal-03011833>**

Submitted on 18 Nov 2020

**HAL** is a multi-disciplinary open access archive for the deposit and dissemination of scientific research documents, whether they are published or not. The documents may come from teaching and research institutions in France or abroad, or from public or private research centers.

L'archive ouverte pluridisciplinaire **HAL**, est destinée au dépôt et à la diffusion de documents scientifiques de niveau recherche, publiés ou non, émanant des établissements d'enseignement et de recherche français ou étrangers, des laboratoires publics ou privés.

# 1 **Evolution-driven versatility of N-terminal acetylation in photoautotrophs**

2 Carmela Giglione<sup>iD,@,1,\*</sup> and Thierry Meinnel<sup>iD,@,1,\*</sup>

3

4

5 <sup>iD</sup>ORCID iD 0002-7475-1558 (C. Giglione); 0000-0001-5642-8637 (T. Meinnel)

6 <sup>@twitter</sup> @giglionelab (C. Giglione); @meinnel (T. Meinnel)

7 <sup>1</sup>Université Paris-Saclay, CEA, CNRS, Institute for Integrative Biology of the Cell (I2BC),

8 91198 Gif-sur-Yvette, France

9 \*Correspondence: carmela.giglione@i2bc.paris-saclay.fr (C. Giglione) or

10 thierry.meinnel@i2bc.paris-saclay.fr (T. Meinnel)

11

12

13 *Keywords:* N-terminal  $\alpha$ -acetyltransferase; lysine  $\varepsilon$ -acetyltransferase; GNAT; plastid; plant

14 development; stress response

15 **ABSTRACT**

16 N-terminal protein  $\alpha$ -acetylation (NTA) is a pervasive protein modification that has recently  
17 attracted renewed interest. Early studies on NTA were mostly conducted in yeast and  
18 metazoans, providing a detailed portrait of the modification, which was indirectly applied to all  
19 eukaryotes. However, new findings originating from photosynthetic organisms have expanded  
20 our knowledge of this modification, revealing strong similarities as well as idiosyncratic  
21 features. Here, we review the most recent advances on NTA and its dedicated machinery in  
22 photosynthetic organisms. We discuss the cytosolic and unique plastid NTA machineries and  
23 their critical biological roles in development, stress responses, protein translocation and  
24 stability. These new findings suggest that the multitasking plastid and cytosolic machineries  
25 evolved to support the specific needs of photoautotrophs.

26

## 27 **N-terminal- $\alpha$ -protein acetylation in brief**

28 N-terminal- $\alpha$ -acetylation (NTA) is the closest but less well-known cousin of lysine- $\epsilon$ -  
29 acetylation (KA). NTA has attracted significant interest over the last decade thanks to a series  
30 of discoveries highlighting its substrates, functions, and modifiers at the molecular, cellular,  
31 and organism levels and its impact on many important cellular functions. Like KA, NTA is an  
32 ubiquitous modification mainly characterized in yeast, humans, insects, and few archaea [1].  
33 NTA is generally regarded as the enzymatic co- or post-translational addition of an acetate  
34 moiety onto protein N- $\alpha$ -amino groups. Although NTA is found in all organisms, the  
35 percentage of proteins undergoing this modification within a proteome increases with organism  
36 complexity, affecting 1-2% of proteins in bacteria [2-4], 10-45% in archaea, 60% in fungi, and  
37 >80% of the cytosolic proteome in multicellular eukaryotes [1, 5].

38

## 39 **Increasing acetylation from photosynthetic bacteria to plants**

### 40 *Cytosolic NTA in photosynthetic eukaryotes*

41 The N-terminal acetylomes of cyanobacteria or green sulfur bacteria have revealed only  
42 a few N-terminal protein acetylation events in photosynthetic bacteria (**Table 1**). By contrast,  
43 the characterization of thousands of N-termini in green algae and land plants (i.e., *Arabidopsis*  
44 *thaliana* or *Populus trichocarpa*) has revealed a cytosolic N-terminal acetylome resembling -  
45 both in terms of extent (~80%) [6] and specificity - the animal acetylome [6-18]. In the diatom  
46 *Thalassiosira pseudonana*, a unicellular photosynthetic eukaryote [19], the N-terminal  
47 acetylome is slightly lower (~70%).

### 48 *Organellar NTA*

49 Although NTA has yet to be detected in mitochondria [20], both co- and post-  
50 translational NTA occur in plastids (Key **Figure 1**). NTA impacts 20-30% of all plastid proteins  
51 [9, 21-23] (**Table 1**). In land plants - where <100 proteins are encoded by the plastid genome

52 and a few dozen have had their N-termini characterized - a significant percentage of plastid-  
53 encoded proteins were N-terminal acetylated (NTAed) (**Table 1**).

54 Extensive N-terminal data are now available describing the major soluble and  
55 membrane complexes of plastids in various organisms (**Table 1**; [18]). NTA is widespread in  
56 major plastid complex subunits but, remarkably, the core translational/transcriptional plastid  
57 machinery is poorly acetylated. This is also true for some complexes including PSI, NDH, or  
58 cytochrome  $b_6f$ , unlike PSII and ATPase, where most major subunits are NTAed. High NTA  
59 levels are similarly observed in the most abundant proteins, namely soluble ribulose-1,5-  
60 biphosphate carboxylase/oxygenase (RuBisCO) complex or insoluble light-harvesting  
61 complex (LHC). These high NTA ratios in plastid protein complexes appear to be unrelated to  
62 the location of protein synthesis, as exemplified by RuBisCO, where each subunit is usually  
63 synthesized in the plastid or nuclear genome. Therefore, high levels of NTAed subunits of some  
64 plastid complexes correlate with oxygenic photosynthesis, which features PSII, RuBisCO, and  
65 the dedicated chlorophyll-binding proteins of LHC. NTA could therefore be related to oxidative  
66 damage and provide an additional mechanism by which plastids can manage oxygen production  
67 whilst preserving redox homeostasis.

68 A main feature of plastid NTA is that acetylation yields (i.e. percentage of NTA of one  
69 single proteoform) are often low [24, 25]. However, this NTA yield might be dependent on  
70 physiological growth conditions including stress, light, and carbon source availability. Full  
71 NTA has only been observed for a few proteins including PSII components such as PsbD and  
72 PsbS, LHC components, amino acid or lipid synthesis enzymes, redox, and a set of plastid  
73 importins (TIC20/55/62, IMB1, SecA [25]). This small set of fully NTAed plastid proteins is  
74 an incomplete characterization, since only a reduced set of plastid proteins have been analyzed.

## 75 **Current state-of-the-art: the plant NAT machinery**

### 76 *General features*

77 NTA is catalyzed by N- $\alpha$ -acetyltransferases (NATs; subunits designated NAAs or  
78 GNATs), which via at least one catalytic subunit transfer the acetyl group from acetyl-CoA to  
79 the free  $\alpha$ -amino groups of protein N-termini. Several cytosolic/membrane NATs have been  
80 identified, each showing distinct substrate specificity [1]. In NatA/B/C/E, the corresponding  
81 catalytic subunit associates with one or more auxiliary subunits to improve catalytic  
82 performance, specificity, and/or ribosome binding [1]. All NAAs belong to the very large  
83 general control non-repressible 5 (GCN5)-related N-acetyltransferase (GNAT) superfamily and  
84 share a common 3D core architecture [26-28]. Recent work has provided a detailed picture of  
85 the NAT machinery in plants. **Table 2** compares the protein entries for *Saccharomyces*  
86 *cerevisiae*, *Homo sapiens*, *Arabidopsis thaliana*, and *Oryza sativa*, which shows that monocots  
87 and dicots display a similar machinery and the same NATs to metazoans except for NAA80,  
88 an actin-specific NAT [1]. Analysis of the machinery of green plants shows strong conservation  
89 in the phylum (**Box 1**).

### 90 *The NatA/NatE core complex*

91 *A. thaliana* NatA was the first NAT complex characterized in a photosynthetic organism  
92 [13, 15]. The core of this complex consists of a catalytically active subunit (AtNAA10) and an  
93 auxiliary subunit AtNAA15 (**Table 2**). Yeast and animal NAA15s serve as ribosome-binding  
94 adaptors and modify NAA10's intrinsic activity [29]. Human NAA10 also exists as a monomer  
95 and, at least *in vitro*, acetylates the  $\alpha$ -amino group of proteins starting with acidic residues  
96 (Asp/Glu) that can be generated post-translationally [30]. However, human and yeast NAA10  
97 do not seem to have intrinsic classical NatA-type activity [29]. In complex with the ribosome-  
98 binding partner NAA15, yeast and human NAA10 display different substrate specificity,  
99 acetylating nascent peptide chains from which the initial methionine (iMet) has been removed

100 by methionine aminopeptidases (MetAPs) during a co-translational process called N-terminal  
101 methionine excision (NME) [31] (**Figure 1**). Due to the substrate specificity of MetAPs, NatA  
102 substrates start with residues featuring non-bulky side chains [32]. Like in humans, NAA10 and  
103 NAA15 are mandatory for NatA activity *in vivo* in *A. thaliana*, affecting 50% of soluble  
104 proteins in leaves [13]. AtNAA15 is anchored to ribosomes [13, 15]. Unlike yeast NatA [33],  
105 AtNAA10-AtNAA15 association is unnecessary for typical AtNatA specificity, preferentially  
106 affecting proteins undergoing NME.

107 In humans and a few fungi, the NatA complex also involves the chaperone Huntingtin-  
108 interacting protein K (HYPK) [34, 35] (**Table 2**). In yeast and metazoans, NatA forms  
109 complexes with another subunit, NAA50 (**Table 2**) [36, 37], defined as NatE [38] and recently  
110 identified in *A. thaliana* [39-41]. AtNAA50 is catalytically active with the cognate NAA50  
111 Met-Leu-Gly-Pro peptide, similar to human NAA50. Unlike yeast and fly NAA50 [28, 36, 42],  
112 AtNAA50 knockout does not affect the NTA of canonical NatA substrates [39]. It was therefore  
113 proposed that (i) the absence of human NAA50 might promote HYPK binding to NatA, which  
114 inhibits NatA activity [34, 35], and/or (ii) human NAA50 might contribute to NatA's ribosomal  
115 association in multicellular eukaryotes [35, 43, 44], although an absence of effects on *A.*  
116 *thaliana* NatA substrates disfavors the second hypothesis. In addition to its NTA activity,  
117 AtNAA50 was shown *in vitro* to auto-acetylate the  $\epsilon$ -amino group of internal lysines (KA  
118 activity), as for HsNAA50 [39]. This dual activity of AtNAA50 seems to fit with its  
119 nucleocytoplasmic and endoplasmic reticulum localization (see below and [39]). It was noticed  
120 that AtNAA50 does not co-immunoprecipitate with AtNatA [40].

### 121 *The NatB complex*

122 In metazoans and yeast, the NatB complex is composed of the catalytic subunit NAA20  
123 and the auxiliary subunit NAA25 [1] (**Table 2**), specifically acetylating the N-termini of Met-  
124 Glu/Asp/Asn/Gln-starting proteins [45]. The first evidence of photosynthetic NatB activity on

125 a Met-Glu substrate was provided by *in vitro* analysis of recombinant AtNAA20 and by  
126 silencing of *NAA25* in tobacco [15]. Plant NatB recapitulates the specificity of NatB in other  
127 organisms [14]. NatB is predicted to contribute 20% of *A. thaliana*'s cytosolic NTAed  
128 proteome.

129 Despite this conserved substrate specificity, only HsNAA20, but not ScNAA20, rescued  
130 NAA20-deficient *A. thaliana naa20-1* lines, suggesting functional assembly with endogenous  
131 AtNAA25 [14].

### 132 *The NatC complex*

133 The NatC complex consists of the catalytic subunit NAA30 and the auxiliary subunits  
134 NAA35 and NAA38 (**Table 2**). NatC acetylates iMet-starting proteins, favoring hydrophobic  
135 and basic amino acids at position 2 in both yeast and humans [46, 47]. However, such proteins  
136 are not systematically NTAed, and other substrate specificity determinants are likely to be  
137 involved downstream of position 2 [48, 49].

138 There is currently no detailed analysis of plant NatC substrate specificity. Nevertheless,  
139 functional complementation of the loss-of-function *mak3* yeast mutant with a putative  
140 AtNAA30 provided evidence that this subunit has NatC activity [50]. NatC activity was  
141 independent of the other two yeast auxiliary subunits, suggesting that AtNAA30 does not  
142 require NatC complex formation for enzymatic activity. However, interaction between  
143 AtNAA30 and AtNAA35, but not two potential NAA38s, was shown [50]. It is likely that the  
144 putative NAA38 subunits were not properly identified in these experiments (see alternative  
145 genes in **Table 2**).

### 146 *NatF/Naa60*

147 NatF is a monomer formed from the sole catalytic subunit NAA60, so far only identified  
148 in multicellular organisms including plants. Five orthologs have been identified in humans,  
149 mainly differing at the N- or C-terminus. Similarly, the three identified *A. thaliana* orthologs



150 differ at their C-terminus. One HsNAA60 isoform is anchored to Golgi membranes [51],  
151 whereas an AtNAA60 isoform showed C-terminal-dependent plasma membrane localization.  
152 It will be interesting to establish how the C-termini of the other two orthologs influence  
153 membrane localization.

154 AtNAA60 showed greater KA activity *in vitro* than HsNAA60. 3D structures of  
155 AtNAA60 in complex with either AcetylCoA or the bisubstrate analogue CoA-Ac-  
156 MetValAsnAlaLeu [52] showed the characteristic folded GNAT architecture with active site  
157 residue arrangements similar to the HsNAA60 structures, including a hydrophobic binding  
158 pocket perfectly matching the high selectivity for iMet. Substitution of conserved residues of  
159 the active site or the substrate-binding pocket of AtNAA60 demonstrated mechanistic  
160 conservation with human NAA50 and NAA60 [52]. Nevertheless, AtNAA60 is monomeric in  
161 solution, whilst HsNAA60 forms a homodimer with acetyl-CoA [53, 54], presumably due to  
162 the difference in the  $\beta 6$ – $\beta 7$  loop region sequence. Finally, N-terminus acetylome profiling of  
163 AtNAA60 KO mutants revealed one plasmodesmata-localized protein, At5g03660, as a  
164 specific AtNAA60 substrate [52].

#### 165 *A plastid-targeted family of active GNATs featuring dual KA and NTA activity*

166 The high frequency of plastid NTA observed in land plants suggests that there is at least  
167 one plastid NAT with large substrate specificity or several isoforms with narrower specificity,  
168 as in the cytosol [9]. Several putative candidates have been proposed in *A. thaliana* and other  
169 land plants, collectively called NatG (see above and [5, 9, 25]). AtGNAT4 (initially called  
170 NAA70, now one of the members of this family) was the first plastid NAT to be characterized  
171 [55]. Characterization of ten putative plastid *A. thaliana* GNAT proteins, including AtGNAT4  
172 [25], revealed that eight were plastid localized and all exhibited the typical GNAT topology but  
173 with several divergences from the cytosolic NAT enzymes [55]. GAP assays [25] revealed  
174 strong NTA activity for six of the eight plastid-associated GNATs (**Box 2**). NTA activity of

175 GNAT1 and GNAT3 was inefficient, most likely because they (i) act on a restricted number of  
176 plastid substrates or (ii) require plant-specific accessory proteins to improve their activity. All  
177 GNAT candidates had a broad range of substrates (**Box 2**). Unexpectedly, all plastid-associated  
178 GNATs displayed specific KA activity, although again this was weak for GNAT1 and GNAT3.  
179 The dual activity of AtGNAT2, also known as NSI (nuclear shuttle interacting), was  
180 demonstrated by AtGNAT2/NSI knockout in two independent backgrounds (*nsi-1* and *nsi-2*)  
181 [25, 56, 57], with global quantitative NTA and KA analyses showing that NTA and KA activity  
182 were affected in AtGNAT2-defective plants. The most sensitive KA and NTA targets in  
183 AtGNAT2-defective plant lines were different, suggesting a different acetylation recognition  
184 mode for each of the two activities. The N-termini NTAs of six major plastid proteins were  
185 affected in the AtGNAT2-defective plant lines (see Table 1 in [25]). Interestingly, NTA of  
186 different N-termini of the same protein were affected in AtGNAT2-defective plant lines,  
187 suggesting long distance contacts between AtGNAT2 and their substrates, perhaps explaining  
188 the specific selectivity of AtGNAT2 for some substrates.

189 GNAT2 was initially described in rice and in *A. thaliana* as a serotonin acetyltransferase  
190 (SNAT1; [58-60]). However, it is a surprisingly weak enzyme, 2-3 orders of magnitude less  
191 active than the mammalian homolog [59]. A second SNAT2 was also identified in rice based  
192 on its close similarity with OsSNAT1 [59], corresponding to AtGNAT1. It is likely that GNATs  
193 of the former SNAT family also display weak activity on small substrates such as serotonin,  
194 highlighting their relaxed specificity. Finally, the plastid-encoded SNAT from the red alga  
195 *Pyropia yezoensis* displays close homology with AtGNAT2 [47] and is most likely a GNAT.

## 196 **Physiological relevance of NATs in phototrophic organisms**

### 197 *The multiple impacts of impaired plant cytosolic machineries*

198 NTA regulates diverse molecular functions in yeast and metazoans [1]. In *A. thaliana*,  
199 *NAA10* and *NAA15* are classified as embryo defective genes [61]. Indeed, characterization of

200 *A. thaliana* T-DNA insertion mutant *NAA10* and *NAA15* lines confirmed that loss of both  
201 subunits arrested embryos at the dermatogen to early globular stage and that AtNatA is required  
202 for the asymmetric division of the hypophysis, root meristem formation, and proper suspensor  
203 development [13, 62, 63]. Additionally, artificial miRNA (*ami*) AtNAA10 and AtNAA15 lines  
204 displayed severe developmental defects and growth retardation compared to wild-type *A.*  
205 *thaliana*, showing that both subunits are necessary for NatA activity. *amiNAA10* and *amiNAA15*  
206 were also highly drought tolerant, presumably due to altered root morphology and reduced  
207 stomatal apertures (**Figure 2**). Given that many drought signaling-associated genes, including  
208 those associated with the phytohormone abscisic acid (ABA), were overexpressed in  
209 *amiNAA10* and *amiNAA15* lines, the extreme drought stress tolerance observed with reduced  
210 NatA activity was ascribed to alterations in ABA perception. Consistent with that hypothesis,  
211 exogenous ABA or drought stress in wild-type plants rapidly depleted NatA transcripts, finally  
212 inducing several adaptive responses that improved plant drought tolerance and survival. No N-  
213 terminal acetylome of drought-stressed plants has yet been reported. However, the use of a  
214 fluorescent probe, which specifically reacts at neutral pH with the N-terminal amino groups of  
215 polypeptides, revealed an increase of free N-termini in response to drought and ABA [13].  
216 Although definitive proof is still missing, these data suggest that the proportion of free N-  
217 termini might also increase in these conditions. Therefore, it was proposed that NTA by NatA  
218 is a hormone-controlled dynamic process that regulates cellular stress responses to drought in  
219 higher plants. How this NTA dynamicity is controlled is unknown. Since the proteasome  
220 machinery was a major upregulated pathway in *amiNAA10* and *amiNAA15*, AtNatA might  
221 control cellular proteostasis.

222 Loss of *A. thaliana* NAA50 function produced dwarf plants with altered root  
223 morphology, infertility, and induced stress signaling responses comparable to the effects of  
224 reduced NatA in plants [15, 39, 40]. Accordingly, reduction of *A. thaliana* NAA50 arrested

225 stem and root growth and senescence and altered developmental process genes and proteins  
226 mediating stress responses [39, 41]. Additionally, reduced AtNAA50 constitutively activated  
227 endoplasmic reticulum (ER) stress signaling, suggesting that AtNAA50 might also play a role  
228 in regulating ER stress in plants (e.g., preventing protein misfolding and/or aggregation).  
229 Interestingly, it has been proposed that indirect AtNAA50-mediated regulation of ER stress is  
230 the primary mechanism responsible for the observed increase in stress signaling in AtNAA50  
231 knockout and knockdown plants (**Figure 2**) [41]. For instance, if NTA is required to prevent  
232 induction of ER stress, then the enhanced resistance to different abiotic stresses may be an  
233 indirect result of changes to ER stress signaling. Although interactions between AtNAA50 and  
234 the *A. thaliana* protein kinase EDR1 (enhanced disease resistance 1), a negative regulator of  
235 cell death during biotic and abiotic stress responses, have been demonstrated, and loss of EDR1  
236 leads to enhanced ER stress sensitivity, how EDR1 in association with AtNAA50 regulates ER  
237 stress is unknown [41].

238 Matsuo et al. [64] first reported photosynthetic NatB in 2012, identifying the catalytic  
239 NatB subunit in *C. reinhardtii* as responsible for the circadian rhythm of rhythm of chloroplast  
240 97 (roc97) mutants. NatB might therefore be essential for maintenance of a robust circadian  
241 clock in *C. reinhardtii*. In *A. thaliana*, AtNatB has been implicated in abiotic stress responses  
242 in addition to playing key roles in vegetative and reproductive developmental processes [14,  
243 65]. Indeed, downregulation of both AtNAA20 or AtNAA25 subunits impacted growth and  
244 resistance to osmotic and high-salt stresses [14]. Finally, a genetic interaction has been  
245 proposed between AtNAA25 and ARGONAUTE10, but the nature of these interactions has not  
246 been established [65].

247 It has also been reported that NatB, by antagonizing NatA, controls the stability of the  
248 immune receptor SUPPRESSOR OF NPR1, CONSTITUTIVE 1 (SNC1) [15]. Indeed, targeted  
249 genetic and biochemical analyses of SNC1 revealed that NatA-mediated acetylation of the N-

250 terminal variant MetMetAsp-SNC1 strongly destabilizes the protein, whereas NatB-mediated  
251 acetylation of the N-terminal variant MetAsp-SNC1 stabilizes the immune receptor (**Figure 2**)  
252 [15]. Therefore, NTA may have opposing effects on a single protein depending on the sequence  
253 context, and the complex regulation afforded by different NAT complexes might provide  
254 flexibility to a specific target protein and faster attainment of appropriate protein concentrations  
255 under dynamic cellular conditions [15, 66-70]. In agreement, NatB-mediated NTA stabilized  
256 SIGMA FACTOR-BINDING PROTEIN 1 (SIB1) [71], a transcription co-regulator targeted to  
257 both the nucleus and chloroplasts. SIB1 is implicated in reactive oxygen species- and salicylic  
258 acid-mediated stress responses and represses the expression of photosynthesis-associated genes  
259 [72, 73].

260         An *A. thaliana* mutant line defective in the NatC component NAA30 was originally  
261 identified based on its photosynthetic phenotype of reduced photosystem II performance [50].  
262 This mutant also exhibited smaller rosettes, paler leaves, and fewer thylakoid complexes  
263 (**Figure 2**). To explain how cytosolic NatC-dependent NTA affected photosynthesis, NTA was  
264 suggested to contribute to the stability and/or import competence of organellar precursor  
265 proteins. Supporting this hypothesis, in Toc-deficient plant lines, NTAed plastid precursor  
266 proteins accumulated in the cytosol [22, 74], and most of these accumulated nuclear-encoded  
267 plastid-imported proteins were found to be NTAed in the cytosol at the level of the N-termini  
268 of uncleaved transit peptides. Therefore, nuclear-encoded plastid-imported proteins might  
269 undergo NTA twice, first in the cytosol during translation and second on neo-N-termini in the  
270 plastid after transit peptide cleavage (**Figure 1**). Consistent with the need for transit peptide  
271 protein modifications before cleavage, cytoplasmic phosphorylation of chloroplast transit  
272 peptides has been shown to be necessary for efficient protein import into the chloroplast [75].  
273 In addition, NTA of the non-cleavable mitochondria-targeting signal of rat chaperonin 10  
274 facilitated mitochondrial import by increasing N-terminal helix stability [76].

275 Depletion of *A. thaliana* NAA60 does not cause any visible phenotype under standard  
276 growth conditions; however, the mutant was hypersensitive to salinity (**Figure 2**), providing  
277 evidence that membrane protein NTA is important during stress [52]. However, how NAA60  
278 contributes to salinity resistance is unknown.

#### 279 *Plastid NTA impairment and its impact on photosynthesis*

280 Our understanding of the physiological relevance of plastid GNATs remains in its  
281 infancy and is made difficult by the partially overlapping and dual NTA and KA activities of  
282 all members. Loss of *A. thaliana* NSI/GNAT2 caused a small reduction in plant growth under  
283 control conditions [56, 57, 77] but severe phenotypes in fluctuating light conditions (**Figure 2**);  
284 NSI/GNAT2 deletion resulted in *A. thaliana* being unable to perform state transitions. Although  
285 LHCII protein phosphorylation/dephosphorylation usually mediates state transitions [78],  
286 LHCII phosphorylation was not impaired in NSI/GNAT2 mutants [56, 57]. KA and NTA  
287 acetylomes revealed that NSI/GNAT2 ablation decreased both plastid KA and NTA [25, 56].  
288 However, GNAT2 inactivation differentially affected its KA and NTA targets with several  
289 photosynthetic apparatus components, including the LCHII subunits only affected in their KA.  
290 This led to the suggestion that GNAT2/NSI KA of LHCII is likely to be the posttranslational  
291 modification required for state transition in *A. thaliana* [56]. The function of GNAT2/NSI-  
292 guided plastid NTA is unknown. Interestingly, *A. thaliana* GNAT2/NSI knockout mutants are  
293 more susceptible to pathogen infection due to its SNAT activity [77]. Although this activity  
294 was only demonstrated for GNAT2/NSI orthologues in rice and not in *A. thaliana*, decreases in  
295 melatonin and salicylic acid levels were observed in *A. thaliana* GNAT/NSI mutant lines.

#### 296 **Concluding remarks and future perspectives**

297 Major efforts are now underway to characterize all the major NAT complexes and NTA  
298 in plants. The available data have already revealed a much more sophisticated NAT machinery  
299 in plants than expected when compared to humans and fungi. Although plants lack the actin-

300 specific NAA80, they all have dedicated NATs – NAA70 and NAA90 - involved in plastid  
301 protein NTA and KA. Within this family, the *Pyropia* GNAT is a plastid remnant evidencing  
302 the endosymbiotic origin of the family. It is therefore unsurprising that cyanobacteria have  
303 specific AtGNAT2 homologs in addition to the usual bacterial-origin NATs, since  
304 photosynthetic bacteria were fully expected to display a dedicated NAT machinery, most likely  
305 for NTA of major PSII subunits (**Table 1**).

306         Plastid NTA is now a major topic in the NAT research field. However, several issues  
307 still need to be addressed. There is a need for dedicated tools to: (i) characterize the specific  
308 acetylome for each GNAT; (ii) uncouple the KA from the NTA activity of each GNAT; and  
309 (iii) discriminate the impact of NTA activity on plastid function from overall cellular functions.  
310 In this respect, it is worth remembering that inhibition of protein N-terminal deacylation - an  
311 organellar co-translational process that can be specifically blocked in plastids - in chlorophyta  
312 and spermatophytes decreases the accumulation of only four plastid proteins, all belonging to  
313 the PSII complex, namely the core protein components PsbA/B/C/D [79-82]. This decreased  
314 stability was hypothesized to be caused by absent NME [81] or the presence of formyl [83], but  
315 the absence of NTA has not yet been excluded even though normal NTA is blocked in the four  
316 destabilized subunits due to deacylation inhibition (**Figure 1**). In addition, the impact of NTA  
317 on directly adjacent Thr phosphorylation has yet to be considered.

318         Partial plastid NTA [24] might occur for a number of reasons. First, the involved  
319 machinery might be poorly efficient due to its post-translational nature in the absence of known  
320 interactions with plastoribosomes. Whether interactions with the ribosome or the import  
321 machinery are via auxiliary subunits or direct will need to be investigated. An absence of  
322 channeling between the substrate and the catalyst at the ribosome, as occurs in the cytosol for  
323 NatA/B/C, could significantly contribute to poor NTA efficiency. Second, plastid NTA might  
324 have initially involved only a few proteins, as in cyanobacteria. The progressive migration of

325 many genes to the nucleus during the course of plastid evolution and the use of an import  
326 machinery leading to transit peptides will have opened up many new, fortuitous targets. As a  
327 result, their NTA would be an unnecessary decoration. If this hypothesis is true, then only fully  
328 NTAed proteins would really matter physiologically, but this also means that this mechanism  
329 would involve significant (and unexpected) AcCoA wastage. Furthermore, LHC components  
330 arising from the nuclear genome appear to display high NTA yields, making this hypothesis  
331 unlikely. Third, plastid protein acetylation might contribute to protein stability/turnover.  
332 Supporting this hypothesis, the chloroplast-encoded AtpE subunit is partially NTAed in several  
333 land plants [84, 85]. Upon drought stress in watermelon, the non-NTAed form of the AtpE  
334 subunit dropped from 72% to 11%, whereas the NTAed form remained constant [84], the  
335 degradation of the former proposed to be mediated by a stress-induced metalloprotease.  
336 Accordingly, short-lived stromal proteins in *C. reinhardtii* were also non-NTAed, which  
337 suggests that NTA promotes plastid protein stability [86]. Alternatively, we propose that plastid  
338 NTA-induced stability is influenced by a combination of modifications. Remember that PSII  
339 turnover often involves vicinal phosphorylation and NTA, as in the case of PsbD in response  
340 to heat or high light stress. Finally, NTAed proteins might be involved in the protein-protein  
341 interactions required in the complexes, whereas the unacetylated isoforms could constitute a  
342 reservoir, progressive acetylation of which would allow post-translational replacement of the  
343 oxygen-damaged proteins. Such recycling without protein neo-synthesis would be well suited  
344 for swift adaptation of plants from low to high light conditions (sunshine/cloudy). Accordingly,  
345 NTA of the PSII and LHCII subunits was recently shown to be crucial for stacking in the  
346 thylakoid membrane [87].

347         The discovery of the association between cytosolic photosynthetic NATs and many  
348 stress-related pathways and retrograde signaling with the plastid machinery opens up new  
349 avenues for studies exploring the molecular mechanisms linking NAT-dependent NTA to plant



350 stress responses and the impact of NTA on communication between different cellular  
351 compartments.

352

### 353 **ACKNOWLEDGEMENTS**

354 This research of the team is funded by the French Agence Nationale de la Recherche (ANR-13-  
355 BSV6-0004, ANR-17-CAPS-0001-01) and has benefited from a French State grant (Saclay  
356 Plant Sciences, reference n° ANR-17-EUR-0007, EUR SPS-GSR) managed by the French  
357 National Research Agency under an Investments for the Future program (reference n° ANR-  
358 11-IDEX-0003-02).

359

### 360 **SUPPLEMENTAL INFORMATION**

361 Supplemental information associated with this article can be found at doi:XXXXXXXX'

362

363 **REFERENCES**

- 364 1. Aksnes, H. et al. (2019) Co-translational, post-translational, and non-catalytic roles of N-  
365 terminal acetyltransferases. *Mol Cell* 73 (6), 1097-1114.
- 366 2. Bienvenut, W.V. et al. (2015) Proteome-wide analysis of the amino terminal status of  
367 *Escherichia coli* proteins at the steady-state and upon deacetylation inhibition. *Proteomics* 15  
368 (14), 2503-18.
- 369 3. Schmidt, A. et al. (2016) The quantitative and condition-dependent *Escherichia coli*  
370 proteome. *Nat Biotechnol* 34 (1), 104-10.
- 371 4. Ouidir, T. et al. (2015) Characterization of N-terminal protein modifications in *Pseudomonas*  
372 *aeruginosa* PA14. *J Proteomics* 114C, 214-225.
- 373 5. Breiman, A. et al. (2016) The intriguing realm of protein biogenesis: Facing the green co-  
374 translational protein maturation networks. *Biochim Biophys Acta* 1864 (5), 531-550.
- 375 6. Liu, C.C. et al. (2013) Identification and analysis of the acetylated status of poplar proteins  
376 reveals analogous N-terminal protein processing mechanisms with other eukaryotes. *PLoS One*  
377 8 (3), e58681.
- 378 7. Martinez, A. et al. (2008) Extent of N-terminal modifications in cytosolic proteins from  
379 eukaryotes. *Proteomics* 8 (14), 2809-2831.
- 380 8. Baerenfaller, K. et al. (2008) Genome-scale proteomics reveals *Arabidopsis thaliana* gene  
381 models and proteome dynamics. *Science* 320 (5878), 938-41.
- 382 9. Bienvenut, W.V. et al. (2012) Comparative large scale characterization of plant versus  
383 mammal proteins reveals similar and idiosyncratic N-alpha-acetylation features. *Mol Cell*  
384 *Proteomics* 11 (6), M111 015131.
- 385 10. Zhang, H. et al. (2018) N-terminomics reveals control of *Arabidopsis* seed storage proteins  
386 and proteases by the Arg/N-end rule pathway. *New Phytol* 218 (3), 1106-1126.
- 387 11. Zhang, H. et al. (2015) Quantitative proteomics analysis of the Arg/N-end rule pathway of  
388 targeted degradation in *Arabidopsis* roots. *Proteomics* 15 (14), 2447-2457.
- 389 12. Venne, A.S. et al. (2015) An improved workflow for quantitative N-terminal charge-based  
390 fractional diagonal chromatography (ChaFRADIC) to study proteolytic events in *Arabidopsis*  
391 *thaliana*. *Proteomics* 15 (14), 2458-69.

- 392 13. Linster, E. et al. (2015) Downregulation of N-terminal acetylation triggers ABA-mediated  
393 drought responses in Arabidopsis. *Nat Commun* 6, 7640.
- 394 14. Huber, M. et al. (2020) NatB-mediated N-terminal acetylation affects growth and abiotic  
395 stress responses. *Plant Physiol* 182, 792-806.
- 396 15. Xu, F. et al. (2015) Two N-terminal acetyltransferases antagonistically regulate the stability  
397 of a nod-like receptor in Arabidopsis. *Plant Cell* 27 (5), 1547-62.
- 398 16. Sun, Q. et al. (2009) PPDB, the Plant Proteomics Database at Cornell. *Nucleic Acids Res*  
399 37 (Database issue), D969-74.
- 400 17. Soh, W.T. et al. (2020) ExteNDing proteome coverage with legumain as a highly specific  
401 digestion protease. *Anal Chem* 92 (4), 2961-2971.
- 402 18. Millar, A.H. et al. (2019) The scope, functions, and dynamics of posttranslational protein  
403 modifications. *Annu Rev Plant Biol* 70, 119-151.
- 404 19. Huesgen, P.F. et al. (2013) Proteomic amino-termini profiling reveals targeting information  
405 for protein import into complex plastids. *PLoS One* 8 (9), e74483.
- 406 20. Giglione, C. and Meinnel, T. (2001) Organellar peptide deformylases: universality of the  
407 N-terminal methionine cleavage mechanism. *Trends Plant Sci.* 6 (12), 566-572.
- 408 21. Zybailov, B. et al. (2008) Sorting signals, N-terminal modifications and abundance of the  
409 chloroplast proteome. *PLoS One* 3 (4), e1994.
- 410 22. Bischof, S. et al. (2011) Plastid proteome assembly without Toc159: photosynthetic protein  
411 import and accumulation of N-acetylated plastid precursor proteins. *Plant Cell* 23 (11), 3911-  
412 28.
- 413 23. Rowland, E. et al. (2015) The Arabidopsis chloroplast stromal N-terminome: complexities  
414 of amino-terminal protein maturation and stability. *Plant Physiol* 169 (3), 1881-96.
- 415 24. Bouchnak, I. and van Wijk, K.J. (2019) N-Degron Pathways in Plastids. *Trends Plant Sci*  
416 24 (10), 917-926.
- 417 25. Bienvenut, W.V. et al. (2020) Dual lysine and N-terminal acetyltransferases reveal the  
418 complexity underpinning protein acetylation. *Mol Syst Biol* 16 (7), e9464.
- 419 26. Vetting, M.W. et al. (2005) Structure and functions of the GNAT superfamily of  
420 acetyltransferases. *Arch Biochem Biophys* 433 (1), 212-26.

- 421 27. Salah Ud-Din, A.I. et al. (2016) Structure and functional diversity of GCN5-related N-  
422 acetyltransferases (GNAT). *Int J Mol Sci* 17 (7), E1018.
- 423 28. Rathore, O.S. et al. (2016) Absence of N-terminal acetyltransferase diversification during  
424 evolution of eukaryotic organisms. *Sci Rep* 6, 21304.
- 425 29. Ree, R. et al. (2018) Spotlight on protein N-terminal acetylation. *Exp Mol Med* 50 (7), 90.
- 426 30. Van Damme, P. et al. (2011) Proteome-derived peptide libraries allow detailed analysis of  
427 the substrate specificities of N(alpha)-acetyltransferases and point to hNaa10p as the post-  
428 translational actin N(alpha)-acetyltransferase. *Mol Cell Proteomics* 10 (5), M110 004580.
- 429 31. Giglione, C. et al. (2015) N-terminal protein modifications: Bringing back into play the  
430 ribosome. *Biochimie* 114, 134-146.
- 431 32. Arnesen, T. et al. (2009) Proteomics analyses reveal the evolutionary conservation and  
432 divergence of N-terminal acetyltransferases from yeast and humans. *Proc Natl Acad Sci U S A*  
433 106 (20), 8157-8162.
- 434 33. Liszczak, G. et al. (2013) Molecular basis for N-terminal acetylation by the heterodimeric  
435 NatA complex. *Nat Struct Mol Biol* 20 (9), 1098-105.
- 436 34. Weyer, F.A. et al. (2017) Structural basis of HypK regulating N-terminal acetylation by the  
437 NatA complex. *Nat Commun* 8, 15726.
- 438 35. Deng, S. et al. (2020) Molecular basis for N-terminal acetylation by human NatE and its  
439 modulation by HYPK. *Nat Commun* 11 (1), 818.
- 440 36. Gautschi, M. et al. (2003) The yeast N(alpha)-acetyltransferase NatA is quantitatively  
441 anchored to the ribosome and interacts with nascent polypeptides. *Mol Cell Biol* 23 (20), 7403-  
442 14.
- 443 37. Evjenth, R. et al. (2009) Human Naa50p (Nat5/San) displays both protein N $\alpha$ - and N $\epsilon$ -  
444 acetyltransferase activity. *J Biol Chem* 284 (45), 31122-31129.
- 445 38. Aksnes, H. et al. (2016) First things first: vital protein marks by N-terminal  
446 acetyltransferases. *Trends Biochem Sci* 41 (9), 746-60.
- 447 39. Armbruster, L. et al. (2020) NAA50 is an enzymatically active N $\alpha$ -acetyltransferase that is  
448 crucial for development and regulation of stress responses. *Plant Physiol* 183(4), 1502-16.

- 449 40. Feng, J. et al. (2020) The N-Terminal acetyltransferase Naa50 regulates Arabidopsis growth  
450 and osmotic stress response. *Plant Cell Physiol* 61 (9), 1565-1575.
- 451 41. Neubauer, M. and Innes, R.W. (2020) Loss of the acetyltransferase NAA50 Induces ER  
452 stress and immune responses and suppresses growth. *Plant Physiol* 183 (4), 1838-1854.
- 453 42. Van Damme, P. et al. (2015) N-terminal acetylome analysis reveals the specificity of Naa50  
454 (Nat5) and suggests a kinetic competition between N-terminal acetyltransferases and  
455 methionine aminopeptidases. *Proteomics* 15 (14), 2436-46.
- 456 43. Knorr, A.G. et al. (2019) Ribosome–NatA architecture reveals that rRNA expansion  
457 segments coordinate N-terminal acetylation. *Nat Struct Mol Biol* 26 (1), 35-39.
- 458 44. Deng, S. et al. (2019) Structure and mechanism of acetylation by the N-terminal dual  
459 enzyme NatA/Naa50 complex. *Structure* 27 (7), 1057-1070.e4.
- 460 45. Van Damme, P. et al. (2012) N-terminal acetylome analyses and functional insights of the  
461 N-terminal acetyltransferase NatB. *Proc Natl Acad Sci U S A* 109 (31), 12449-54.
- 462 46. Polevoda, B. et al. (1999) Identification and specificities of N-terminal acetyltransferases  
463 from *Saccharomyces cerevisiae*. *EMBO J* 18 (21), 6155-6168.
- 464 47. Van Damme, P. et al. (2016) A role for human N-alpha Acetyltransferase 30 (Naa30) in  
465 maintaining mitochondrial integrity. *Mol Cell Proteomics* 15 (11), 3361-3372.
- 466 48. Kimura, Y. et al. (2003) N-Terminal modifications of the 19S regulatory particle subunits  
467 of the yeast proteasome. *Arch Biochem Biophys* 409 (2), 341-348.
- 468 49. Starheim, K.K. et al. (2009) Knockdown of human N alpha-terminal acetyltransferase  
469 complex C leads to p53-dependent apoptosis and aberrant human Arl8b localization. *Mol Cell*  
470 *Biol* 29 (13), 3569-81.
- 471 50. Pesaresi, P. et al. (2003) Cytoplasmic N-terminal protein acetylation is required for efficient  
472 photosynthesis in Arabidopsis. *Plant Cell* 15 (8), 1817-32.
- 473 51. Aksnes, H. et al. (2017) Molecular determinants of the N-terminal acetyltransferase Naa60  
474 anchoring to the Golgi membrane. *J Biol Chem* 292 (16), 6821-6837.
- 475 52. Linster, E. et al. (2020) The Arabidopsis N $\alpha$ -acetyltransferase NAA60 locates to the plasma  
476 membrane and is vital for the high salt stress response. *New Phytol* 228 (2), 554-569.

- 477 53. Chen, J.Y. et al. (2016) Structure and function of human Naa60 (NatF), a Golgi-localized  
478 bi-functional acetyltransferase. *Sci Rep* 6, 31425.
- 479 54. Støve, S.I. et al. (2016) Crystal structure of the Golgi-associated human N $\alpha$ -  
480 acetyltransferase 60 reveals the molecular determinants for substrate-specific acetylation.  
481 *Structure* 24 (7), 1044-56.
- 482 55. Dinh, T.V. et al. (2015) Molecular identification and functional characterization of the first  
483 N $\alpha$ -acetyltransferase in plastids by global acetylome profiling. *Proteomics* 15 (14), 2426-  
484 35.
- 485 56. Koskela, M.M. et al. (2018) Chloroplast acetyltransferase NSI is required for state  
486 transitions in *Arabidopsis thaliana*. *Plant Cell* 30 (8), 1695-1709.
- 487 57. Koskela, M.M. et al. (2020) Comparative analysis of thylakoid protein complexes in state  
488 transition mutants *nsi* and *stn7*: focus on PSI and LHCII. *Photosynth Res* 145 (1), 15-30.
- 489 58. Kang, K. et al. (2013) Molecular cloning of rice serotonin N-acetyltransferase, the  
490 penultimate gene in plant melatonin biosynthesis. *J Pineal Res* 55 (1), 7-13.
- 491 59. Byeon, Y. et al. (2016) Cloning and characterization of the serotonin N-acetyltransferase-2  
492 gene (SNAT2) in rice (*Oryza sativa*). *J Pineal Res* 61 (2), 198-207.
- 493 60. Lee, H.Y. et al. (2014) Cloning of *Arabidopsis* serotonin N-acetyltransferase and its role  
494 with caffeic acid O-methyltransferase in the biosynthesis of melatonin in vitro despite their  
495 different subcellular localizations. *J Pineal Res* 57 (4), 418-426.
- 496 61. Devic, M. (2008) The importance of being essential: EMBRYO-DEFECTIVE genes in  
497 *Arabidopsis*. *C R Biol* 331 (10), 726-36.
- 498 62. Feng, J. et al. (2016) Protein N-terminal acetylation is required for embryogenesis in  
499 *Arabidopsis*. *J Exp Bot* 67 (15), 4779-89.
- 500 63. Feng, J. and Ma, L. (2016) NatA is required for suspensor development in *Arabidopsis*.  
501 *Plant Signal Behav* 11 (10), e1231293.
- 502 64. Matsuo, T. et al. (2012) N-terminal acetyltransferase 3 gene is essential for robust circadian  
503 rhythm of bioluminescence reporter in *Chlamydomonas reinhardtii*. *Biochem Biophys Res*  
504 *Commun* 418 (2), 342-346.

- 505 65. Ferrandez-Ayela, A. et al. (2013) Mutation of an Arabidopsis NatB N-alpha-terminal  
506 acetylation complex component causes pleiotropic developmental defects. PLoS One 8 (11),  
507 e80697.
- 508 66. Kapos, P. et al. (2015) N-terminal modifications contribute to flowering time and immune  
509 response regulations. Plant Signal Behav 10 (10), e1073874.
- 510 67. Gibbs, D.J. (2015) Emerging functions for N-terminal protein acetylation in plants. Trends  
511 Plant Sci 20 (10), 599-601.
- 512 68. Linster, E. and Wirtz, M. (2018) N-terminal acetylation: an essential protein modification  
513 emerges as an important regulator of stress responses. J Exp Bot 69 (19), 4555-4568.
- 514 69. Gibbs, D.J. et al. (2016) From start to finish: amino-terminal protein modifications as  
515 degradation signals in plants. New Phytol 211 (4), 1188-94.
- 516 70. Varshavsky, A. (2019) N-degron and C-degron pathways of protein degradation. Proc Natl  
517 Acad Sci U S A 116 (2), 358-366.
- 518 71. Li, Z. et al. (2020) N-terminal acetylation stabilizes SIGMA FACTOR BINDING  
519 PROTEIN 1 involved in salicylic acid-primed cell death. Plant Physiol 183 (1), 358-370.
- 520 72. Lai, Z. et al. (2011) Arabidopsis sigma factor binding proteins are activators of the  
521 WRKY33 transcription factor in plant defense. Plant Cell 23 (10), 3824-41.
- 522 73. Lv, R. et al. (2019) Uncoupled expression of nuclear and plastid photosynthesis-associated  
523 genes contributes to cell death in a lesion mimic mutant. Plant Cell 31 (1), 210-230.
- 524 74. Köhler, D. et al. (2015) Characterization of chloroplast protein import without Tic56, a  
525 component of the 1-Megadalton translocon at the inner envelope membrane of chloroplasts.  
526 Plant Physiol 167 (3), 972-990.
- 527 75. Waagemann, K. and Soll, J. (1996) Phosphorylation of the transit sequence of chloroplast  
528 precursor proteins. J Biol Chem 271 (11), 6545-54.
- 529 76. Jarvis, J.A. et al. (1995) Solution structure of the acetylated and noncleavable mitochondrial  
530 targeting signal of rat chaperonin 10. J Biol Chem 270 (3), 1323-31.
- 531 77. Lee, H.Y. et al. (2015) Arabidopsis serotonin N-acetyltransferase knockout mutant plants  
532 exhibit decreased melatonin and salicylic acid levels resulting in susceptibility to an avirulent  
533 pathogen. J Pineal Res 58 (3), 291-9.

534 78. Pietrzykowska, M. et al. (2014) The light-harvesting chlorophyll a/b binding proteins Lhcb1  
535 and Lhcb2 play complementary roles during state transitions in *Arabidopsis*. *Plant Cell* 26 (9),  
536 3646-60.

537 79. Serero, A. et al. (2001) Distinctive features of the two classes of eukaryotic peptide  
538 deformylases. *J Mol Biol* 314 (4), 695-708.

539 80. Dirk, L.M. et al. (2001) Eukaryotic peptide deformylases. Nuclear-encoded and chloroplast-  
540 targeted enzymes in *Arabidopsis*. *Plant Physiol* 127 (1), 97-107.

541 81. Giglione, C. et al. (2003) Control of protein life-span by N-terminal methionine excision.  
542 *EMBO J* 22 (1), 13-23.

543 82. Moon, S. et al. (2008) Rice peptide deformylase PDF1B is crucial for development of  
544 chloroplasts. *Plant Cell Physiol* 49 (10), 1536-46.

545 83. Piatkov, K.I. et al. (2015) Formyl-methionine as a degradation signal at the N-termini of  
546 bacterial proteins. *Microb Cell* 2 (10), 376-393.

547 84. Hoshiyasu, S. et al. (2013) Potential involvement of N-terminal acetylation in the  
548 quantitative regulation of the  $\epsilon$  subunit of chloroplast ATP synthase under drought stress. *Biosci*  
549 *Biotechnol Biochem* 77 (5), 998-1007.

550 85. Schmidt, C. et al. (2017) Acetylation and phosphorylation control both local and global  
551 stability of the chloroplast F(1) ATP synthase. *Sci Rep* 7, 44068.

552 86. Bienvenut, W.V. et al. (2011) Dynamics of post-translational modifications and protein  
553 stability in the stroma of *Chlamydomonas reinhardtii* chloroplasts. *Proteomics* 11 (9), 1734-50.

554 87. Albanese, P. et al. (2020) How paired PSII-LHCII supercomplexes mediate the stacking of  
555 plant thylakoid membranes unveiled by structural mass-spectrometry. *Nat Commun* 11 (1),  
556 1361.

557 88. Deng, S. and Marmorstein, R. Protein N-Terminal Acetylation: Structural Basis,  
558 Mechanism, Versatility, and Regulation. *Trends in Biochemical Sciences*.

559 89. Vener, A.V. et al. (2001) Mass spectrometric resolution of reversible protein  
560 phosphorylation in photosynthetic membranes of *Arabidopsis thaliana*. *J Biol Chem* 276 (10),  
561 6959-6966.



- 562 90. Gomez, S.M. et al. (2002) The chloroplast grana proteome defined by intact mass  
563 measurements from liquid chromatography mass spectrometry. *Mol Cell Proteomics* 1 (1), 46-  
564 59.
- 565 91. Turkina, M.V. et al. (2006) Environmentally modulated phosphoproteome of  
566 photosynthetic membranes in the green alga *Chlamydomonas reinhardtii*. *Mol Cell Proteomics*  
567 5 (8), 1412-25.
- 568 92. Baniulis, D. et al. (2009) Structure-function, stability, and chemical modification of the  
569 cyanobacterial cytochrome b<sub>6</sub>f complex from *Nostoc* sp. PCC 7120. *J Biol Chem* 284 (15),  
570 9861-9869.
- 571 93. Guskov, A. et al. (2009) Cyanobacterial photosystem II at 2.9-Å resolution and the role of  
572 quinones, lipids, channels and chloride. *Nat Struct Mol Biol* 16 (3), 334-342.
- 573 94. Broser, M. et al. (2010) Crystal Structure of Monomeric Photosystem II from  
574 *Thermosynechococcus elongatus* at 3.6-Å Resolution. *J Biol Chem* 285 (34), 26255-26262.
- 575 95. Yang, M.-k. et al. (2014) Proteogenomic analysis and global discovery of posttranslational  
576 modifications in prokaryotes. *Proc Natl Acad Sci U S A* 111 (52), E5633-E5642.
- 577 96. Houtz, R.L. et al. (1992) Posttranslational Modifications in the Amino- Terminal Region of  
578 the Large Subunit of Ribulose- 1,5-Bisphosphate Carboxylase/Oxygenase from Several Plant  
579 Species. *Plant Physiol* 98 (3), 1170-1174.
- 580 97. Pfefferkorn, B. and Meyer, H.E. (1986) N-terminal amino acid sequence of the Rieske iron-  
581 sulfur protein from the cytochrome b<sub>6</sub>/f-complex of spinach thylakoids. *FEBS Lett* 206 (2),  
582 233-237.
- 583 98. Pierre, Y. et al. (1995) Purification and characterization of the cytochrome *b<sub>6</sub>f* complex  
584 from *Chlamydomonas reinhardtii*. *J Biol Chem* 270 (49), 29342-29349.
- 585 99. Kouyianou, K. et al. (2012) Proteome profiling of the green sulfur bacterium  
586 *Chlorobaculum tepidum* by N-terminal proteomics. *Proteomics* 12 (1), 63-7.
- 587 100. Misumi, O. et al. (2005) *Cyanidioschyzon merolae* genome. A tool for facilitating  
588 comparable studies on organelle biogenesis in photosynthetic eukaryotes. *Plant Physiol* 137 (2),  
589 567-585.

- 590 101. Zhao, Y.-P. et al. (2019) Resequencing 545 ginkgo genomes across the world reveals the  
591 evolutionary history of the living fossil. *Nat Commun* 10 (1), 4201.
- 592 102. Li, F.-W. et al. (2018) Fern genomes elucidate land plant evolution and cyanobacterial  
593 symbioses. *Nat Plants* 4 (7), 460-472.
- 594 103. Zhang, L. et al. (2019) The water lily genome and the early evolution of flowering plants.  
595 *Nature* 577 (7788), 79-84.
- 596 104. Grzela, R. et al. (2017) The C-terminal residue of phage Vp16 PDF, the smallest peptide  
597 deformylase, acts as an offset element locking the active conformation. *Sci Rep* 7 (1), 11041.
- 598 105. Colaert, N. et al. (2009) Improved visualization of protein consensus sequences by  
599 iceLogo. *Nat Methods* 6 (11), 786-7.
- 600
- 601

602 **FIGURES**

603 **Key Figure 1. Main pathways leading to protein acetylation in plants.** In photosynthetic  
604 organisms, NTA occurs in all cellular compartments where there is protein synthesis, except  
605 for mitochondria. In the cytoplasm, NTA is ensured by different NAT classes (A/B/C/E/F).  
606 NatE is made of NatA subunits (NAA10/NAA25) plus NAA50 (see Figure 4C in Ref.[88]).  
607 Although NAA40 has not yet been characterized in plants, *A. thaliana* histones H4 and H2A  
608 have similar N-termini as in fungi and humans suggesting similar function. Moreover, GNAT8  
609 and GNAT9, initially identified as putative plastid NATs, were finally observed to localize to  
610 the cytoplasm and, in the case of GNAT8, the nucleus [25]. Seven additional GNATs  
611 (GNAT1/2/3/4/5/7/10) have been shown to localize to plastids and display dual NTA and KA  
612 activities [25]. GNAT6 is associated with both the outer side of the chloroplasts and the nucleus  
613 [25]. (1), (2), or (3) following a given catalyst indicates that the reaction is performed with  
614 various enzymes and the number refers to the order. SPP and TPP are plastid signal and transit  
615 peptide peptidase, respectively. Fo is N-formyl. This figure was created using BioRender  
616 (<https://biorender.com/>).

617

618 **Figure 2. Summary of the physiological impact of different characterized plant NATs.**  
619 Cartoon summarizing the main effects reported in the text. The same color code as in **Figure 1**  
620 is used to refer to the different NATs or NAAs.

621

622  
623

**Table 1. Compilation of the protein acetylation status in plastid major complexes in various photosynthetic organisms<sup>a</sup>**

Function/complex	Photosynthetic organism	NTAed subunits	UnNTAed subunits	% of the complex that contain NTAed proteins	Refs <sup>b</sup>
<b>NDH</b>	<i>A. thaliana</i>	Ndh45	NdhA/B/C/D/E/F/G/H/I/J/K/S/U	7%	[17, 23]
<b>PSI</b>	<i>A. thaliana</i>	PsaA	Psab/C/E/G/I/J/T	14%	[9, 17, 23]
	<i>T. pseudonana</i>	PsaD	PsaA/B/C/F/L	17%	[19]
<b>PSII</b>	<i>A. thaliana</i>	PsbA/B/C/D/F/H/J/L/Q/S	PsbE/I/K/M/N/O/T/Z	56%	[9, 17, 21-23, 25, 89, 90]
	<i>P. sativum</i>	PsbA/B/D/F/J/T	PsbE/H/L/M/T/Z	50%	[87] <sup>#</sup>
	<i>T. pseudonana</i>	PsbC/D/F/L	PsbB/E	67%	[19]
	<i>C. reinhardtii</i>	PsbA/C/D	PsbE		[91]
	<i>Nostoc</i>	PsbF/J			[92]
	<i>Synechococcus</i>	PsbD/F/J			[93-95]
<b>ATPase</b>	<i>A. thaliana</i>	AtpA/B/E/H	AtpD/F/I	57%	[23]
	<i>S. oleracea</i>	AtpA/B/E			[85]
	<i>T. pseudonana</i>	AtpA	AtpD/H	33%	[19]
	<i>C. reinhardtii</i>	AtpA/B/E	AtpI	75%	<sup>b</sup>
<b>RuBisCO</b>	<i>A. thaliana</i>	RbcL, RbcS		100%	[9, 23]
	<i>M. polymorpha</i>	RbcL			[96]
	<i>T. pseudonana</i>	RbcL			[19]
	<i>C. reinhardtii</i>	RbcL			[96]
<b>LHC</b>	<i>A. thaliana</i>	Lhc2.1/2.2/3.1/4/6, Lhc13.1, Lhb1b2, Cp24	Lhc1/2/3, Lhb1b1, Cp26	62%	[17]
	<i>P. sativum</i>	Lhcb1/2/4.2/4.3/5	Lhcb3/6	71%	[87]
	<i>C. reinhardtii</i>	Lhcb4, Lhcbm4/6/9			[91]
	<i>T. pseudonana</i>	Lhcf2/5/7/9/11, Lher2, Lhcx2	Lher3/4/11/14, lhcf10, fcp2/10	50%	[19]
<b>Ribosome</b>	<i>A. thaliana</i>	Rpl2/5/15/34, Rps5/9/15	Rps2/3/4/7/8/11/12/13/14/15/16/17/18/19/21, Rpl1/2/3/4/6/12/13/14/16/19/20/21/22/23/32/33/36	17%	[17, 23]
	<i>S. oleracea</i>		rpl2/14/16/20/22/23/32/33/36;rps2/3/4/7/8/11/1/14/19	0%	<sup>b</sup>
	<i>T. pseudonana</i>	Rpl23	Rps2/3/4/7/8/11/12/13/14/15/16/17/18/19/21, Rpl1/2/3/4/6/12/13/14/16/19/20/21/22/23/32/33/36	17%	[19]
<b>CYT b6f</b>	<i>A. thaliana</i>		PetA/B/D/G/L/N	0%	[9, 17, 21, 23]
	<i>S. oleracea</i>		PetC		[97]
	<i>T. pseudonana</i>	PetB/C	PetA/D		[19]
	<i>C. reinhardtii</i>		PetA/C/M		[98]
	<i>Nostoc</i>	PetC			[92]
<b>CLP</b>	<i>A. thaliana</i>	ClpP1/3/5, ClpT1	ClpP6, ClpT2	67%	[17, 23]
	<i>T. pseudonana</i>	ClpB1			[19]
<b>RNA polymerase</b>	<i>A. thaliana</i>		RpoA/B/C1/C2	0%	[23]
	<i>Zea maize</i>		RpoB/C1/C2	0%	<sup>b</sup>
<b>Other functions</b>	<i>A. thaliana</i>	Tic214, DnaJ	MatK, Orf77		[23]
	<i>C. tepidum</i>	Q8KD44, Q8KFS3, Q8KE86, Q8KAU3, Q8KAL6			[99]
	<i>T. pseudonana</i>		DnaK, GroL, ThiG, Ycf39, Ycf46	0%	[19]

624  
625

<sup>a</sup> Proteins can arise from both plastid and nuclear genomes. References are indicated. A database compiling *A. thaliana* and other land plant data is available at NTerDB at

626 <https://energiome.i2bc.paris-saclay.fr/> [18]. NDH is for NADPH dehydrogenase, CYT for  
627 Cytochrome and CLP for ATP-dependent caseinolytic protease.

628 <sup>b</sup> See table available at <https://www.i2bc.paris-saclay.fr/spip.php?article1261>. The  
629 corresponding references are detailed at <https://www.i2bc.paris-saclay.fr/spip.php?article1262>.

630

631 **Table 2. Plant NAA and NAT complexes<sup>a</sup>**

Cell localization	Organism		<i>S. cerevisiae</i> (Yeast)	<i>H. sapiens</i> (Human)	<i>A. thaliana</i>	<i>O. sativa</i> (Rice)	
	Complex	Subunit	Accession number	Accession number	Gene No	Gene No	
Cytosol	NatA/E	NAA10	P07347	P41227	At5g13780	Os04g0635800	
		NAA11 <sup>b</sup>	NR	Q9BSU3	NR	NR	
		NAA15 <sup>c</sup>	P12945	Q9BXJ9	At1g80410	Os01g0617500	
		NAA16 <sup>c,d</sup>	NR	Q6N069	NR	NR	
		HYPK <sup>c</sup>	NR	Q9NX55	At3g06610 <sup>f</sup>	Os03g61680 <sup>f</sup>	
		NAA50 <sup>e</sup>	Q08689	Q9GZZ1	At5g11340	P0410E03.23	
	NatB	NAA20	Q06504	P61599	At1g03150	Os11g32280	
		NAA25 <sup>c</sup>	Q12387	Q14CX7	At5g58450	Os05g0345400	
	NatC	NAA30	Q03503	Q147X3	At2g38130	Os11g32280	
		NAA35 <sup>c</sup>	Q02197	Q5VZE5	At2g11000	P0689B12.25	
		NAA38 <sup>c</sup>	P23059	O95777	At4g18372 <sup>f</sup>	Os06g0677600 <sup>f</sup>	
	NatD	NAA40	Q04751	Q86UY6	At1g18335	Os05g0387800	
NatF	NAA60	NR	Q9H7X0	At5g16800	B1053A04.3		
NatH	NAA80	NR	Q93015	NR	NR		
-	GNAT8	NR	NR	At2g39020	Os03g05710		
-	GNAT9	NR	NR	At2g04845	OsJ_09757		
Plastid	NatG <sup>g</sup>	NAA90	GNAT1	NR	NR	At1g26220	Os08g0102000
			GNAT2/NSI	NR	NR	At1g32070	Os05g0481000
			GNAT3	NR	NR	At4g19985	LOC4339320
		NAA70	GNAT4	NR	NR	At2g39000	Os02g0806000
			GNAT5	NR	NR	At1g24040	Os04g0465500
			GNAT6	NR	NR	At2g06025	LOC4331807
			GNAT7	NR	NR	At4g28030	B1015H11.141
			GNAT10	NR	NR	At1g72030	Os07g0264800

632 <sup>a</sup> Each entry is indicated for all NAAs from *S. cerevisiae*, *H. sapiens*, *A. thaliana*, and *O. sativa*.

633 <sup>b</sup> Duplicated version, alternative to NAA10

634 <sup>c</sup> Auxiliary subunit, without catalytic activity

635 <sup>d</sup> Duplicated version, alternative to NAA15

636 <sup>e</sup> Inactive in *S. cerevisiae*, where it acts as sheer auxiliary subunit

637 <sup>f</sup> Remains to be validated experimentally

638 <sup>g</sup> No evidence for the formation of a complex built with various GNAT subunits. Globally refers to plastid NTA (NAA70 and NAA90 families, see **Box 1**).

639 NR, not relevant, means that the corresponding orthologous component was not identified.

640

641

642 **BOXES**

643 **Box 1: Evolutionary boundaries of NAAs across the plant kingdom**

644 The Nat machinery varies across the various clades and orders of the plant kingdom,  
645 which includes algae and land plants (**Figure IA**). NAAs all share the dedicated GNAT family  
646 structural domain involved in acetyl-CoA binding (domain architecture ID 11418877) and they  
647 are usually associated with the RimI-conserved domain (COG0456). **Figure IA** is a phylogram  
648 constructed from 179 NAA orthologs found in 13 representative species for which robust  
649 genome and/or proteome annotation were available in each clade. The updated phylogram adds  
650 new key species such as the red alga *Cyanidioschyzon merolae* [100], the living fossil  
651 gymnosperm maidenhair tree *Ginkgo biloba* [101], the small fern fairy moss *Azolla filiculoides*  
652 [102], and the magnoliids water lily *Nymphaea colorata* [103] (**Figure IB**). Remarkably, all  
653 plants, from algae to dicots, show very similar features. First, they all display NAA10/20/30/40.  
654 NAA50 could not be retrieved in red algae, whereas NAA60 could not be identified in algae.  
655 Second, GNAT4 orthologs could be retrieved in all species (**Figure IB**). As suggested in [25],  
656 it is clear that GNAT5/6/7 and GNAT10 are closely related to GNAT4 (NAA70s) and might  
657 have resulted from progressive gene duplication, as observed in many plant genomes. This does  
658 not necessarily imply that they do not display their own specificity or exhibit differences, as  
659 illustrated in **Figure ID**. Nevertheless, not all representatives of the kingdom contain all  
660 members. Red algae, which have a reduced proteome, contain only GNAT4; all GNAT4-related  
661 proteins were included in the same subfamily (NAA70; **Table 2**). Similarly, as GNAT1/2/3 are  
662 closely related, they were proposed to belong to the same subfamily, NAA90 (**Table 2**). At  
663 least one NAA90 family ortholog is present in all representative members of the plant kingdom.  
664 GNAT8, previously predicted to be a plastid NAT but finally described as a cytosolic protein  
665 [25], has only been identified in land plants, in contrast to GNAT9, which has been identified

666 in all plants except red algae. GNAT9 was reported to more closely resemble the RimJL family  
667 (COG1670) [25].

668 Therefore, in plants, the minimal machinery consists of one copy of cytosolic  
669 NAA10/20/30/40 and of the plastid-targeted subfamilies NAA70 and NAA90. This is the case  
670 for red algae, which lack NAA50, NAA60 as well as both GNAT8 and GNAT9.

671

672 **Box 1, Figure I. Photosynthetic organisms express a large array of NATs, including**  
673 **plastid-specific isoforms.** Most data are available at UniProt  
674 (<https://www.uniprot.org/proteomes/>), the algal genomics resource at the JGI  
675 (<https://mycocosm.jgi.doe.gov/phyocosm/home>) and, when missing, dedicated resources  
676 (e.g., <http://cyanophora.rutgers.edu/cyanophora>).

677 (A) Organisms used to sample the green NAA landscape and their positions with respect to  
678 eukaryotic evolution. 13 organisms were selected to cover and evenly sample the diversity of  
679 photosynthetic eukaryotic proteomes. The figure with the tree of plants according to the  
680 Haeckel tree of life (1866). Each proteome was screened from data mostly available in UniProt  
681 reference proteomes (<https://www.uniprot.org/proteomes/>). PSI-BLAST analysis was  
682 systematically performed at NCBI (<https://blast.ncbi.nlm.nih.gov/>) to identify annotated  
683 homologs. TBLASTN was also searched as required. (B) 176 sequences were selected to  
684 represent the sequence diversity of the catalytic subunits of NATs among photosynthetic  
685 species. The sequences were aligned, and the bootstrap tree was constructed as previously  
686 described [104]. Internal values labeled on each node record the stability of the branch over the  
687 1,000 bootstrap replicates. The figure displays a simplified representation of the tree. All data,  
688 distance, and entry numbers are available upon request. The NAA-60 nomenclature is similar  
689 to that [1] (see also **Table 2**).



690 **Box 2. Assessing NAT substrate specificity**

691 The development of the global acetylation profiling (GAP) assay has been instrumental for  
692 assessing NTA activity and substrate specificity of plant NATs [55]. The GAP assay is based  
693 on the expression of putative NAAs in *E. coli*, taking advantage of the low level of NTAed  
694 proteins in *E. coli* and exploiting a dedicated protocol for the enrichment, identification, and  
695 quantification of NTAed N-termini. Using this assay, expression of AtNAA10 in *E. coli* [55]  
696 recapitulated plant selectivity as deduced directly by comparison of wild-type acetylation and  
697 NatA knockdown plant lines [13]. **Figure I** illustrates how both approaches - which compile  
698 data from dozens of acetylated and non-acetylated proteins - are complementary and reveal  
699 that: (i) Ser-starting proteins are the best substrates for AtNAA10 (GAP assay, **Figure IB**); (ii)  
700 Ala-starting proteins are the most sensitive to AtNatA downregulation (**Figure IA**); and (iii)  
701 there is high counter-selection against Met-starting proteins. Why *A. thaliana* AtNAA15 does  
702 not contribute to AtNAA10 selectivity as much as in other organisms is currently unclear.

703 N-terminomics global analysis based on *A. thaliana* lines exhibiting reduced NatB  
704 levels [14] revealed a clear preference for AtNatB towards N-termini retaining their iMet  
705 followed by Asp and Glu and, to a smaller extent, Asn (**Figure IC**).

706 Additionally, a GAP assay with AtNAA50 revealed it had broad substrate specificity  
707 for N-termini, partially overlapping with human NAA50 substrate specificity (see online  
708 supplemental information **Figure S1A**) [39]. GAP assaying of AtNAA60 [52] revealed  
709 substrate specificity comparable to that of HsNAA60, with a preference for an iMet and a highly  
710 variable position 2 (see online supplemental information **Figure S1B**).

711 GNATs have relaxed specificity. This relaxed NTA substrate specificity was mainly  
712 dependent on the amino acids at positions 1, 2, and 3 (**Figure ID**). For instance, all of the six  
713 most active plastid AtGNATs were very efficient with N-termini starting with an iMet but  
714 showed clear differences induced by the position 2 amino acid. GNAT1 was the only GNAT

715 that efficiently acetylated Met-Met substrates, and GNAT10 was more prone to acetylating N-  
716 termini starting with a Met, showing similar substrate specificity to NatC/E/F and to a lesser  
717 extent NatB-like substrates. GNAT2, 4, 5, and 7 acted more efficiently on NatA-like substrates,  
718 albeit with different impact depending on the amino acid at position 2 (**Figure I D**).

719 **Box 2, Figure I. Hints towards the substrate specificity of the main *A. thaliana* NATs.**

720 Protein logo representations in panels A-C were displayed using iceLogo [105]. Positive and  
721 negative sets were used to compare NTAed *vs.* non-NTAed positions in the mutant plant lines  
722 or NTAed *vs.* non-NTAed positions recovered from the GAP assay. Unlike a classic logo,  
723 iceLogo reveals favored and disfavored positions whilst masking positions that are neutral as  
724 equally occurring in both sets. (A) Specificity of AtNatA as deduced from (NAA10+NAA15)  
725 knockdown in Arabidopsis. N-terminomics data from *amiNAA10* and *amiNAA15* knockdown  
726 plant lines (available in [13]). The positive set includes 108 N-termini, which were significantly  
727 decreased upon reduced expression of NatA (i.e., >20%) in either or both lines; the negative set  
728 includes 220 N-termini modified below 5%. (B) AtNAA10 specificity as deduced from the  
729 GAP assay. Data are from [55]. The same cutoffs as in (A) were used to define the positive (45  
730 N-termini) and negative sets (92). (C) Same as (A) but with NatB in *naa20-1* and *naa20-2* T-  
731 DNA insertion mutant lines exhibiting reduced NatB expression [14]. 28 positives *vs.* 57  
732 negatives were used to build the iceLogo. Data are from [14]. (D) Unique and redundant  
733 substrate specificity of plastid AtGNATs. The data were compiled from [25]. The data of the  
734 acetylation yield resulting from global acetylome profiling of the six more significant plastid  
735 AtGNATs are reported in each column. All protein substrates starting with the same first two  
736 amino acids are considered as identical, and the upper value of acetylation yield is reported.  
737 Amino acids at position two are grouped according to the chemical properties of their side-  
738 chains. Acetylation yield is reported and associated with a color code where red and blues  
739 indicate the highest and lowest levels, respectively. The first two amino acids of NAT substrates

740 are reported in the first two columns. A value of x means x% of the retrieved *E. coli* proteins  
741 starting with amino acids y are NTAed if GNATz is expressed.  
742

743 **GLOSSARY**

744 **Acetylation yield:** one single protein may feature *in vivo* both unmodified (free) and N-  
745 acetylated termini resulting in partial *in vivo* NTA. The acetylation yield corresponds to the  
746 NTAed/(Free+NTAed) fraction. A fully NTAed protein displays a 100% yield whereas a fully  
747 unmodified protein has a 0% yield. The yield value ranges 0 to 100.

748 **General control non-repressible 5 (GCN5)-related N-acetyltransferases (GNATs):** a  
749 superfamily of N-acetyltransferases using acetyl CoA as the acetyl donor and a number of small  
750 or larger molecules as acceptors.

751 **Global acetylation profiling (GAP) assay:** N-terminomics analysis of *E. coli* proteins after  
752 expression of a catalytically active NAA. Allows unbiased quantification and assessment of the  
753 NTA yields of dozens of random substrates simultaneously. Reveals substrate selectivity of the  
754 studied NAA by comparing NTAed to non-NTAed proteins.

755 **Huntingtin interacting protein K (HYPK):** a protein that protects against Huntingtin polyQ-  
756 mediated apoptosis and regulates the NatA/E complex.

757 **N-Acetylated at the aminotermminus (NTAed):** refers to a protein that is acetylated on its N-  
758 terminal amino group. This NTA can be partial (see Acetylation yield)

759 **N-terminal  $\alpha$ -acetylation (NTA):** co- and post-translational modification consisting of the  
760 addition of an acetyl group to the positively charged free  $\alpha$ -amino group of the first amino acid  
761 of proteins.

762 **N-terminal methionine excision process (NME):** co-translational modification involving  
763 deformylation by peptide deformylases (PDFs) in mitochondria and chloroplasts and  
764 methionine aminopeptidases (MetAPs) in all cellular compartments where protein synthesis  
765 occurs. NME consists of the sequential trimming of the first Met (iMet or FormylMet) from  
766 nascent chains.

767 **N-terminal acetyltransferase (NAT):** enzyme belonging to the GNAT superfamily that  
768 catalyzes NTA, composed of a catalytic subunit (NAA) that can be associated with one or more  
769 auxiliary subunits.

770 **Light-harvesting complex (LHC)** (or antenna supercomplex): a complex formed from a large  
771 number of protein subunits and chlorophyll molecules embedded in the thylakoid membrane of  
772 plants. It collects sunlight and transfers it to photosystems.

773 **Lysine  $\epsilon$ -acetylation (KA):** reversible post-translational modification involving the transfer of  
774 an acetyl group from a donor (e.g., acetyl CoA or acetyl phosphate) to  $\epsilon$ -amino groups of  
775 lysines.

776 **Lysine  $\epsilon$ -acetyltransferase (KAT):** enzyme controlling KA. KATs belong to four families:  
777 P300/CBP, MYST, GNAT, or YoJ.

778 **Photosystem II (PSII):** multi-subunit pigment-protein complex embedded in the thylakoid  
779 membranes of all oxygenic photosynthetic organisms that catalyzes the oxidation of water using  
780 solar energy. Some microorganisms like Chlorobi (*Chlorobium tepidum*) do not use PSII.

781 **Plastid:** organelle found in the cells of plants, algae, and some other eukaryotic organisms (e.g.,  
782 parasites such as Apicomplexa) originating from cyanobacteria endosymbiosis into other  
783 primitive eukaryotic cells.

784 **Ribulose-1,5-bisphosphate carboxylase/oxygenase (RuBisCO):** a highly abundant stromal  
785 complex made of eight large catalytic (RbcL) subunits and eight small regulatory (RbcS)  
786 subunits. It is primarily involved in CO<sub>2</sub> assimilation into most organic compounds. It also  
787 displays photorespiration activity.

788 **Serotonin acetyltransferase (SNAT):** an enzyme that catalyzes the rate-limiting step of  
789 melatonin synthesis, the N-acetylation of serotonin to N-acetylserotonin.

## **HIGHLIGHTS**

- The identification and characterization of the cytosolic and plastid NAT machinery has revealed the importance of NTA in plant development, responses to abiotic stresses, immunity, and protein translocation and stability.
- A unique plastid NAT machinery has now been identified and characterized.
- Several NATs show dual KA and NTA activities, including plastid forms.
- There is strong conservation of the entire machinery across the Viridiaeplanta phylum.
- Plastid photoxygenic autotrophy-dedicated machineries such as RuBisCO, LHC, or PSII display significantly more frequent NTA of their subunits.

## OUTSTANDING QUESTIONS

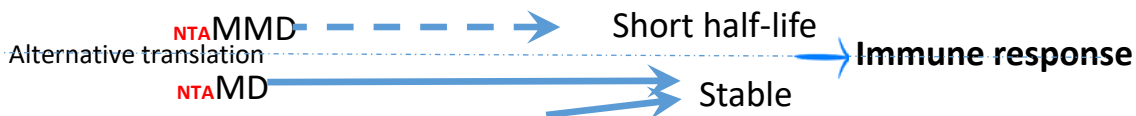
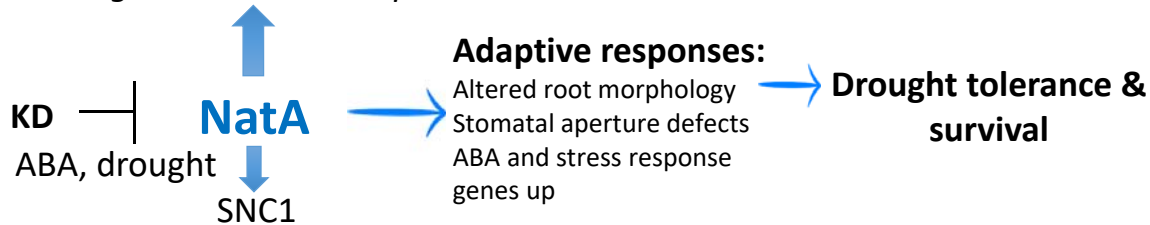
- Why does *A. thaliana* AtNAA15 not contribute to AtNAA10 selectivity as much as in other organisms?
- What is the real nature of the NatA/E complex in photosynthetic organisms? Do NatA and NatE independently exist or do they actually belong to the same complex?
- Are the free Naa10 or Naa50 catalytic subunits of photosynthetic organisms active *in vivo* like in metazoans? Do they exhibit KA, NTA, or both activities, and in which compartment(s)? Characterization of the putative plant HYPK will help to clarify the dialogue between NAA50 and other NatA subunits.
- What molecular mechanisms underpin the effect of cytosolic NATs on abiotic and biotic stress responses? Are NTA dynamics influenced by other factors such as stresses or dialogues with other modifications?
- How do the different C-termini of AtNAA60 influence membrane localization?
- Does NatA- and NatB-induced NTA trigger generally opposing effects on protein turnover?
- Do plant NAA40s also specifically acetylate - like in fungi and humans - histone variants H2A and H4 starting with SGRK? Are plant NAA40s also both nuclear and cytosolic?
- Which proteolytic machineries are involved in NatA-dependent protein turnover, including SNC1?
- What is the impact of cytosolic and plastid NATs on N-degrons?
- How and why do NAAs achieve both KA and NTA activities?
- What are the specificity determinants for KA activity?
- What does NTA add to the biology of the major photooxygenic autotrophy complexes in plants including LHC, PSII, and RuBisCO?
- Why are so many plastid proteins only partially acetylated?

- Why are there so many different GNATs in plastids? Is this due to redundancy, the specific functions of each, or both?
- Do plastid GNATs act within higher complexes together or with auxiliary proteins like the major cytosolic NATs? Which ones act co-translationally on plastid-encoded proteins and post-translationally on imported proteins?

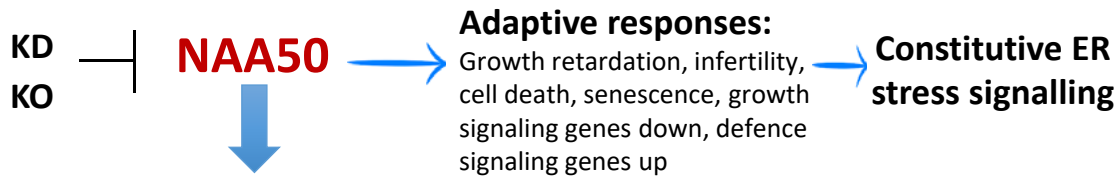




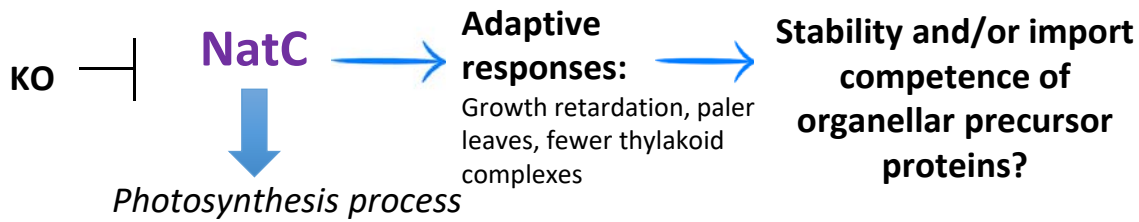
*Normal growth and development*



*Normal growth, development, circadian clock*



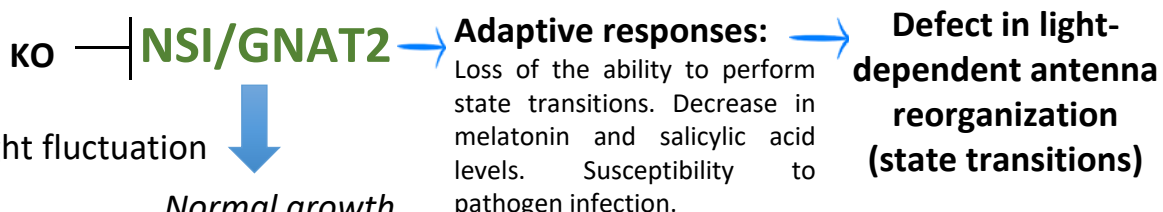
*Normal growth and development*



*Photosynthesis process*

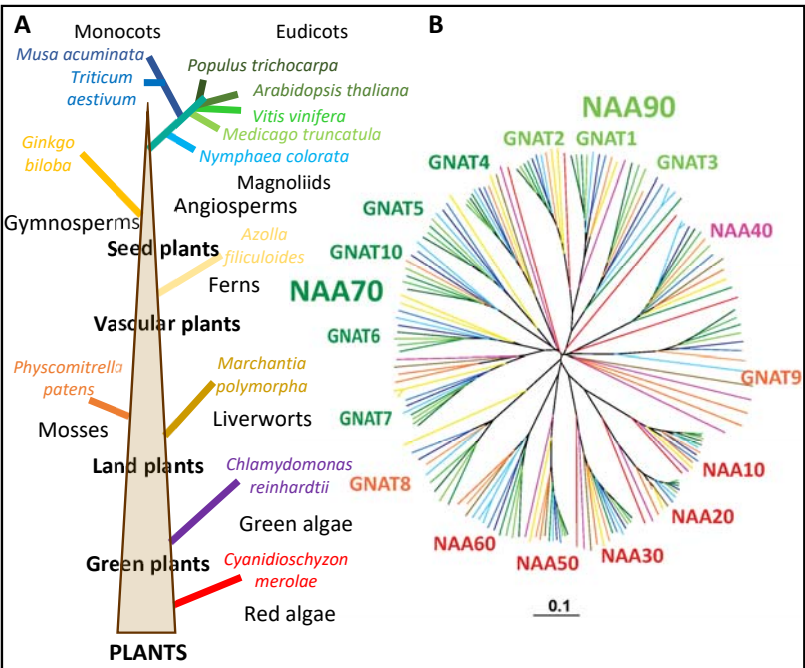


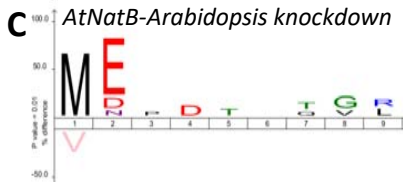
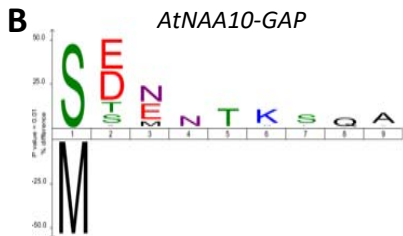
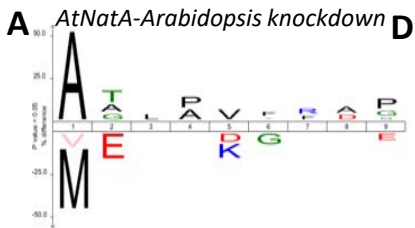
*Specific for membrane proteins*



Light fluctuation

*Normal growth*





<b>GNAT</b>		2	4	5	6	7	10
<i>aa1</i>	<i>aa2</i>						
<b>Ala</b>	AGST	100	44	30	25	35	30
	DE	31	99	95	65	50	29
	K	34	57	76	52	26	
	ILMV	97	100	99	100	37	97
	NQ	98	100	25		5	4
FY		99	77	14	27		
<b>Gly</b>	T		19				
<b>Ile</b>	K						6
<b>Met</b>	GST		12	95	45	76	100
	DE	61	100	81	99	71	33
	HK	55	27	35	94	96	55
	ILVM	92	91	97	100	94	94
	NQ	100	100	50	100	99	50
	FY	27	18	100	100	56	93
<b>Pro</b>	L					90	
	S					5	
<b>Ser</b>	ACST	46	100	89	88	67	52
	DE	94	59	15	20	65	27
	K	6	29		9	16	17
	ILMV	29	100	62	65	11	14
	NQ	83	99	99	55	30	77
	F	7		34	31		
<b>Thr</b>	AST	+	+		61		
	DE	32	23	98	20	82	7
	KR		12			86	
	ILMV	97	96	98	100	58	16
	NQ	100	99	5	24	99	
	F			+	34	15	28
<b>Val</b>	AS	13	+	+	99	96	
	D	94	95		87	87	96
	K					78	
	WY	48	12	12	5	58	9

## Evolution-driven versatility of N-terminal acetylation in photoautotrophs

Carmela Giglione<sup>1,\*</sup> and Thierry Meinzel<sup>1,\*</sup>

<sup>1</sup>Université Paris-Saclay, CEA, CNRS, Institute for Integrative Biology of the Cell (I2BC), 91198 Gif-sur-Yvette, France

\*Correspondence: [carmela.giglione@i2bc.paris-saclay.fr](mailto:carmela.giglione@i2bc.paris-saclay.fr) (C. Giglione) or [thierry.meinzel@i2bc.paris-saclay.fr](mailto:thierry.meinzel@i2bc.paris-saclay.fr) (T. Meinzel)

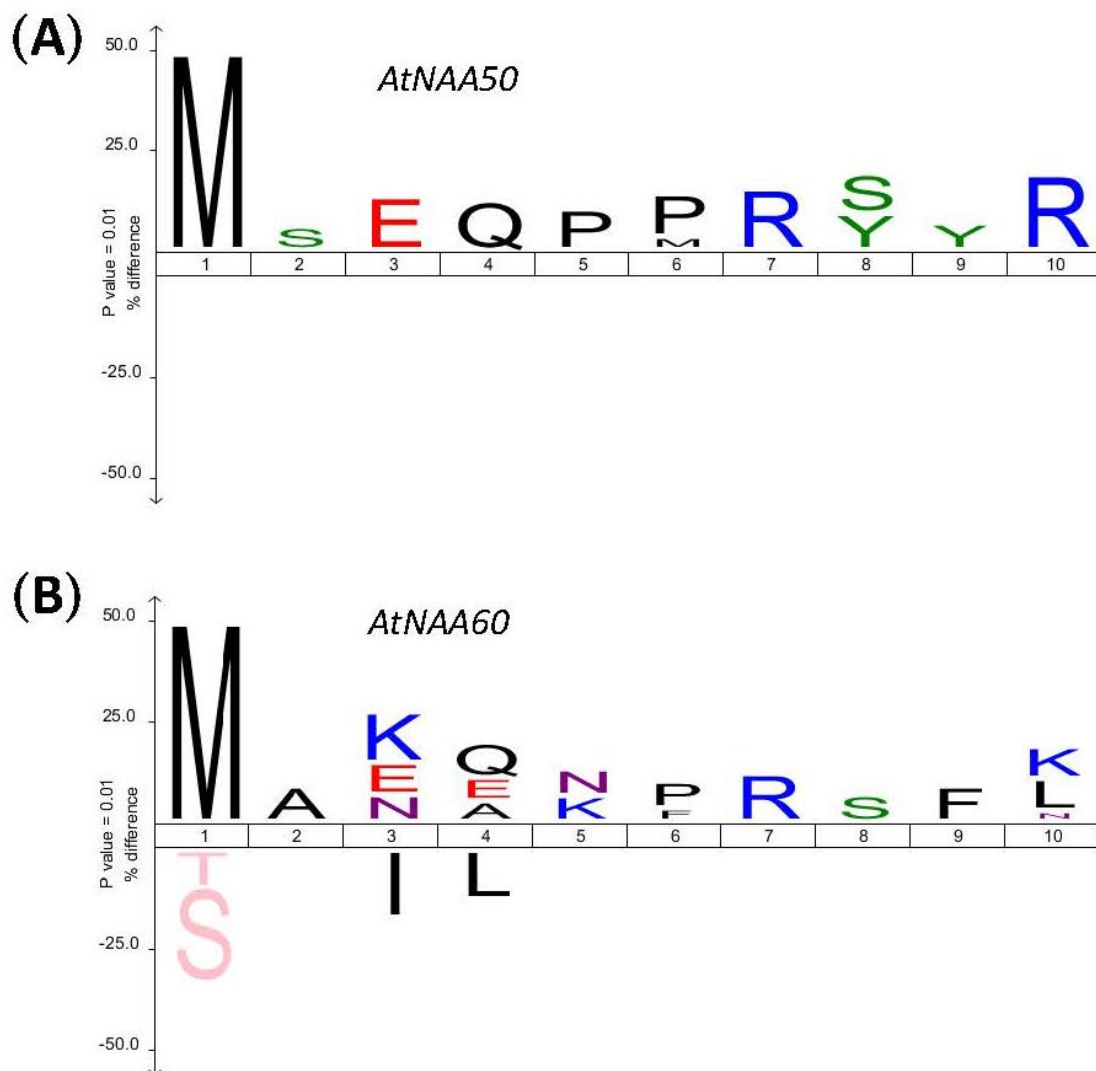


**Figure S1. Substrate selectivity of *Arabidopsis* NAA50 and NAA60.** GAP assays were performed with (A) AtNAA50 and (B) NAA60. Data are from [39, 52] The same cutoffs as in **Figure 2** were used to define the positive (19 and 68 N-termini, respectively) and negative (106 and 130, respectively) sets in either panel.